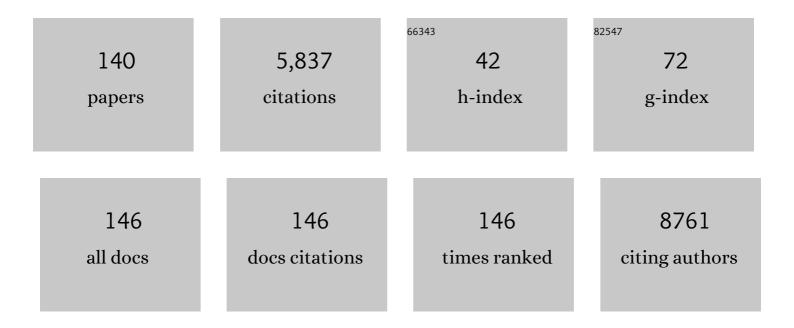
## Yang Yang Li

List of Publications by Year in descending order

Source: https://exaly.com/author-pdf/9170126/publications.pdf Version: 2024-02-01



#	Article	IF	CITATIONS
1	Biomolecular screening with encoded porous-silicon photonic crystals. Nature Materials, 2002, 1, 39-41.	27.5	395
2	Toward Practical Highâ€Arealâ€Capacity Aqueous Zincâ€Metal Batteries: Quantifying Hydrogen Evolution and a Solidâ€Ion Conductor for Stable Zinc Anodes. Advanced Materials, 2021, 33, e2007406.	21.0	382
3	Polymer Replicas of Photonic Porous Silicon for Sensing and Drug Delivery Applications. Science, 2003, 299, 2045-2047.	12.6	367
4	Hierarchical Composite Electrodes of Nickel Oxide Nanoflake 3D Graphene for Highâ€Performance Pseudocapacitors. Advanced Functional Materials, 2014, 24, 6372-6380.	14.9	210
5	Nitrogen-Doped Nanoporous Carbon Membranes with Co/CoP Janus-Type Nanocrystals as Hydrogen Evolution Electrode in Both Acidic and Alkaline Environments. ACS Nano, 2017, 11, 4358-4364.	14.6	199
6	Ultrathin Cu <sub>2</sub> O as an efficient inorganic hole transporting material for perovskite solar cells. Nanoscale, 2016, 8, 6173-6179.	5.6	191
7	Electrochemical doping of anatase TiO <sub>2</sub> in organic electrolytes for high-performance supercapacitors and photocatalysts. Journal of Materials Chemistry A, 2014, 2, 229-236.	10.3	172
8	A facile method to improve the high rate capability of Co3O4 nanowire array electrodes. Nano Research, 2010, 3, 895-901.	10.4	165
9	Rapid Microwave Synthesis of Porous TiO <sub>2</sub> Spheres and Their Applications in Dye-Sensitized Solar Cells. Journal of Physical Chemistry C, 2011, 115, 10419-10425.	3.1	111
10	Integration of nano-Al with Co3O4 nanorods to realize high-exothermic core–shell nanoenergetic materials on a silicon substrate. Combustion and Flame, 2012, 159, 2202-2209.	5.2	91
11	Triple-layer Fabry-Perot absorber with near-perfect absorption in visible and near-infrared regime. Optics Express, 2013, 21, 25307.	3.4	89
12	Vapor Sensors Based on Optical Interferometry from Oxidized Microporous Silicon Films. Langmuir, 2002, 18, 2229-2233.	3.5	88
13	Fe <sub>1â^'x</sub> S/C nanocomposites from sugarcane waste-derived microporous carbon for high-performance lithium ion batteries. Green Chemistry, 2016, 18, 3029-3039.	9.0	83
14	Self-ordered Nanotubular TiO2 Multilayers for High-Performance Photocatalysts and Supercapacitors. Electrochimica Acta, 2016, 203, 257-264.	5.2	78
15	CsPbl <sub>3</sub> /PbSe Heterostructured Nanocrystals for High-Efficiency Solar Cells. ACS Energy Letters, 2020, 5, 2401-2410.	17.4	77
16	Highly Stable Porous Silicon–Carbon Composites as Label-Free Optical Biosensors. ACS Nano, 2012, 6, 10546-10554.	14.6	76
17	Facile synthesis and electrochemical characterization of porous and dense TiO2 nanospheres for lithium-ion battery applications. Journal of Power Sources, 2011, 196, 6394-6399.	7.8	75
18	pH-triggered release of vancomycin from protein-capped porous silicon films. Nanomedicine, 2008, 3, 31-43	3.3	74

#	Article	IF	CITATIONS
19	Low-temperature fabrication of brown TiO <sub>2</sub> with enhanced photocatalytic activities under visible light. Chemical Communications, 2016, 52, 2988-2991.	4.1	71
20	Rare earth-free composites of carbon dots/metal–organic frameworks as white light emitting phosphors. Journal of Materials Chemistry C, 2019, 7, 2207-2211.	5.5	68
21	Construction of FeP Hollow Nanoparticles Densely Encapsulated in Carbon Nanosheet Frameworks for Efficient and Durable Electrocatalytic Hydrogen Production. Advanced Science, 2019, 6, 1801490.	11.2	68
22	Growth of TiO2 nanorod arrays on reduced graphene oxide with enhanced lithium-ion storage. Journal of Materials Chemistry, 2012, 22, 19061.	6.7	65
23	A Zn–nitrite battery as an energy-output electrocatalytic system for high-efficiency ammonia synthesis using carbon-doped cobalt oxide nanotubes. Energy and Environmental Science, 2022, 15, 3024-3032.	30.8	65
24	Anodic nanoporous SnO2 grown on Cu foils as superior binder-free Na-ion battery anodes. Journal of Power Sources, 2016, 307, 634-640.	7.8	64
25	Porous TiO <sub>2</sub> Photonic Band Gap Materials by Anodization. Journal of Physical Chemistry C, 2012, 116, 5509-5515.	3.1	61
26	Hydrogen-Location-Sensitive Modulation of the Redox Reactivity for Oxygen-Deficient TiO <sub>2</sub> . Journal of the American Chemical Society, 2019, 141, 8407-8411.	13.7	59
27	Thermal evaporation-induced anhydrous synthesis of Fe3O4–graphene composite with enhanced rate performance and cyclic stability for lithium ion batteries. Physical Chemistry Chemical Physics, 2013, 15, 7174.	2.8	58
28	One-pot scalable synthesis of Cu–CuFe <sub>2</sub> O <sub>4</sub> /graphene composites as anode materials for lithium-ion batteries with enhanced lithium storage properties. Journal of Materials Chemistry A, 2014, 2, 13892.	10.3	56
29	Dramatic improvement enabled by incorporating thermal conductive TiN into Si-based anodes for lithium ion batteries. Energy Storage Materials, 2020, 29, 367-376.	18.0	55
30	TiO <sub>2</sub> Nanotube Array/Monolayer Graphene Film Schottky Junction Ultraviolet Light Photodetectors. Particle and Particle Systems Characterization, 2013, 30, 630-636.	2.3	53
31	Polymer-pyrolysis assisted synthesis of vanadium trioxide and carbon nanocomposites as high performance anode materials for lithium-ion batteries. Journal of Power Sources, 2014, 261, 184-187.	7.8	52
32	An Alumina-Coated Fe3O4-Reduced Graphene Oxide Composite Electrode as a Stable Anode for Lithium-ion Battery. Electrochimica Acta, 2015, 156, 147-153.	5.2	52
33	Interface-based tuning of Rashba spin-orbit interaction in asymmetric oxide heterostructures with 3d electrons. Nature Communications, 2019, 10, 3052.	12.8	51
34	Facile fabrication of N/S-doped carbon nanotubes with Fe <sub>3</sub> O <sub>4</sub> nanocrystals enchased for lasting synergy as efficient oxygen reduction catalysts. Journal of Materials Chemistry A, 2017, 5, 13189-13195.	10.3	50
35	Thermal and Nonthermal Effects in Plasmonâ€Mediated Electrochemistry at Nanostructured Ag Electrodes. Angewandte Chemie - International Edition, 2020, 59, 6790-6793.	13.8	49
36	Tuning the Bi <sup>3+</sup> -photoemission color over the entire visible region by manipulating secondary cations modulation in the ScV <sub>x</sub> P <sub>1â^'x</sub> O <sub>4</sub> :Bi <sup>3+</sup> (0 ≤i>x ≤) solid solution. Journal of Materials Chemistry C, 2019, 7, 9865-9877.	5.5	48

#	Article	IF	CITATIONS
37	TiO2 nanotube-based field effect transistors and their application as humidity sensors. Materials Research Bulletin, 2012, 47, 54-58.	5.2	47
38	Multicolor Tuning and Temperature-Triggered Anomalous Eu <sup>3+</sup> -Related Photoemission Enhancement via Interplay of Accelerated Energy Transfer and Release of Defect-Trapped Electrons in the Tb <sup>3+</sup> ,Eu <sup>3+</sup> -Doped Strontium–Aluminum Chlorites. ACS Applied Materials & Interfaces, 2018, 10, 36157-36170.	8.0	47
39	A Facile Strategy to Construct Silverâ€Modified, ZnOâ€Incorporated and Carbonâ€Coated Silicon/Porousâ€Carbon Nanofibers with Enhanced Lithium Storage. Small, 2019, 15, e1900436.	10.0	47
40	Influence of modification method and transition metal type on the physicochemical properties of MCM-41 catalysts and their performances in the catalytic ozonation of toluene. Applied Catalysis B: Environmental, 2011, 107, 245-252.	20.2	45
41	Scalable synthesis of Fe3O4 nanoparticles anchored on graphene as a high-performance anode for lithium ion batteries. Journal of Solid State Chemistry, 2013, 201, 330-337.	2.9	43
42	Observation of superconductivity in structure-selected Ti2O3 thin films. NPG Asia Materials, 2018, 10, 522-532.	7.9	43
43	Defective Black TiO <sub>2</sub> Nanotube Arrays for Enhanced Photocatalytic and Photoelectrochemical Applications. ACS Applied Nano Materials, 2019, 2, 7372-7378.	5.0	43
44	Lamellarly Stacking Porous N, P Coâ€Doped Mo <sub>2</sub> C/C Nanosheets as High Performance Anode for Lithiumâ€Ion Batteries. Small, 2019, 15, e1805022.	10.0	43
45	Anodic Synthesis of Hierarchical SnS/SnO <i><sub>x</sub></i> Hollow Nanospheres and Their Application for Highâ€Performance Naâ€Ion Batteries. Advanced Functional Materials, 2019, 29, 1901000.	14.9	43
46	From Titanium Sesquioxide to Titanium Dioxide: Oxidation-Induced Structural, Phase, and Property Evolution. Chemistry of Materials, 2018, 30, 4383-4392.	6.7	42
47	Electronic-reconstruction-enhanced hydrogen evolution catalysis in oxide polymorphs. Nature Communications, 2019, 10, 3149.	12.8	42
48	Ag <sub>2</sub> S Quantum Dots as an Infrared Excited Photocatalyst for Hydrogen Production. ACS Applied Energy Materials, 2019, 2, 2751-2759.	5.1	40
49	Facile Synthesis of Nitrogenâ€Rich Carbon Dots as Fertilizers for Mung Bean Sprouts. Advanced Sustainable Systems, 2019, 3, 1800132.	5.3	40
50	Evaporation-induced synthesis of carbon-supported Fe3O4 nanocomposites as anode material for lithium-ion batteries. CrystEngComm, 2013, 15, 1324.	2.6	38
51	Periodic porous silicon thin films with interconnected channels as durable anode materials for lithium ion batteries. Materials Chemistry and Physics, 2014, 144, 25-30.	4.0	38
52	Titanium dioxide nanomaterials for photocatalysis. Journal Physics D: Applied Physics, 2017, 50, 193003.	2.8	37
53	Forming a Highly Active, Homogeneously Alloyed AuPt Co-catalyst Decoration on TiO <sub>2</sub> Nanotubes Directly During Anodic Growth. ACS Applied Materials & Interfaces, 2018, 10, 18220-18226.	8.0	37
54	Novel porous silicon vapor sensor based on polarization interferometry. Sensors and Actuators B: Chemical, 2002, 87, 58-62.	7.8	34

#	Article	IF	CITATIONS
55	Selective Removal of the Outer Shells of Anodic TiO <sub>2</sub> Nanotubes. Small, 2013, 9, 37-44.	10.0	34
56	In situ reduction of silver nanoparticles on hybrid polydopamine–copper phosphate nanoflowers with enhanced antimicrobial activity. Journal of Materials Chemistry B, 2017, 5, 5311-5317.	5.8	34
57	Mesoporous C-coated SnO <sub>x</sub> nanosheets on copper foil as flexible and binder-free anodes for superior sodium-ion batteries. Journal of Materials Chemistry A, 2017, 5, 2243-2250.	10.3	33
58	Gold Nanoparticle-Decorated Silver Needle for Surface-Enhanced Raman Spectroscopy Screening of Residual Malachite Green in Aquaculture Products. ACS Applied Nano Materials, 2019, 2, 2752-2757.	5.0	33
59	UiO-66-NO <sub>2</sub> as an Oxygen "Pump―for Enhancing Oxygen Reduction Reaction Performance. Chemistry of Materials, 2019, 31, 1646-1654.	6.7	33
60	High-performance supercapacitors based on amorphous C-modified anodic TiO2 nanotubes. Applied Surface Science, 2016, 362, 399-405.	6.1	31
61	Two-Dimensional Cobalt Phosphate Hydroxide Nanosheets: A New Type of High-Performance Electrocatalysts with Intrinsic CoO <sub>6</sub> Lattice Distortion for Water Oxidation. ACS Applied Materials & Interfaces, 2019, 11, 38633-38640.	8.0	31
62	Rugated porous Fe3O4 thin films as stable binder-free anode materials for lithium ion batteries. Journal of Materials Chemistry, 2012, 22, 22692.	6.7	30
63	Self-Cleaning Organic Vapor Sensor Based on a Nanoporous TiO2 Interferometer. ACS Applied Materials & Interfaces, 2012, 4, 4177-4183.	8.0	30
64	Reproducible and recyclable SERS substrates: Flower-like Ag structures with concave surfaces formed by electrodeposition. Applied Surface Science, 2015, 333, 126-133.	6.1	30
65	Mesoporous SnO <sub>2</sub> Nanostructures of Ultrahigh Surface Areas by Novel Anodization. ACS Applied Materials & Interfaces, 2016, 8, 28862-28871.	8.0	30
66	Water-enabled crystallization of mesoporous SnO <sub>2</sub> as a binder-free electrode for enhanced sodium storage. Journal of Materials Chemistry A, 2017, 5, 23967-23975.	10.3	30
67	Simple Designed Micro–Nano Si–Graphite Hybrids for Lithium Storage. Small, 2021, 17, e2006373.	10.0	26
68	Insertable and reusable SERS sensors for rapid on-site quality control of fish and meat products. Chemical Engineering Journal, 2021, 426, 130733.	12.7	26
69	Painting a rainbow on silicon - a simple method to generate a porous silicon band filter gradient. Physica Status Solidi (A) Applications and Materials Science, 2005, 202, 1616-1618.	1.8	25
70	Electrochemical dealloying using pulsed voltage waveforms and its application for supercapacitor electrodes. Journal of Power Sources, 2014, 257, 374-379.	7.8	25
71	Synthesis of g-C <sub>3</sub> N <sub>4</sub> /Silica Gels for White-Light-Emitting Devices. Particle and Particle Systems Characterization, 2017, 34, 1600258.	2.3	25
72	Bottom-up synthesis of iron and nitrogen dual-doped porous carbon nanosheets for efficient oxygen reduction. Chemical Communications, 2019, 55, 5789-5792.	4.1	25

#	Article	IF	CITATIONS
73	Synthesis of Mesoporous ZIFâ€8 Nanoribbons and their Conversion into Carbon Nanoribbons for Highâ€Performance Supercapacitors. Chemistry - A European Journal, 2018, 24, 11185-11192.	3.3	24
74	Design of Fe,N co-doped multi-walled carbon nanotubes for efficient oxygen reduction. Chemical Communications, 2020, 56, 14467-14470.	4.1	24
75	Selective electrodeposition of Ni into the intertubular voids of anodic TiO <sub>2</sub> nanotubes for improved photocatalytic properties. Journal of Materials Research, 2013, 28, 405-410.	2.6	20
76	A feasible approach toward bioactive glass nanofibers with tunable protein release kinetics for bone scaffolds. Colloids and Surfaces B: Biointerfaces, 2014, 122, 785-791.	5.0	20
77	Hydrothermal preparation of hierarchical MoS2-reduced graphene oxide nanocomposites towards remarkable enhanced visible-light photocatalytic activity. Ceramics International, 2017, 43, 2384-2388.	4.8	20
78	Plasmonic metal nanostructures: concepts, challenges and opportunities in photo-mediated chemical transformations. IScience, 2021, 24, 101982.	4.1	19
79	Morphology Control of Anodic TiO2 Nanomaterials via Cold Work Pretreatment of Ti Foils. Journal of the Electrochemical Society, 2011, 158, C346.	2.9	18
80	Electrochemical fabrication and optical properties of periodically structured porous Fe2O3 films. Electrochemistry Communications, 2012, 20, 178-181.	4.7	18
81	Dense Alkyne Arrays of a Zr(IV) Metal–Organic Framework Absorb Co <sub>2</sub> (CO) <sub>8</sub> for Functionalization. Inorganic Chemistry, 2020, 59, 5626-5631.	4.0	18
82	Metal-Based Photonic Coatings from Electrochemical Deposition. Journal of the Electrochemical Society, 2009, 156, D508.	2.9	16
83	Fe,N Co-Doped Mesoporous Carbon Nanosheets for Oxygen Reduction. ACS Applied Nano Materials, 2020, 3, 5637-5644.	5.0	16
84	Nickel nanotube array via electroplating and dealloying. Thin Solid Films, 2018, 658, 1-6.	1.8	15
85	<i>&gt;g</i> <sub>3</sub> N <sub>4</sub> â€Modified Waterâ€Crystallized Mesoporous SnO <sub>2</sub> for Enhanced Photoelectrochemical Properties. Particle and Particle Systems Characterization, 2018, 35, 1800155.	2.3	14
86	Controlling Plasmon-Aided Reduction of <i>p</i> -Nitrothiophenol by Tuning the Illumination Wavelength. ACS Catalysis, 2021, 11, 14898-14905.	11.2	14
87	An anti-freezing biomineral hydrogel of high strain sensitivity for artificial skin applications. Nano Research, 2022, 15, 6655-6661.	10.4	14
88	Mineral Hydrogel from Inorganic Salts: Biocompatible Synthesis, Allâ€inâ€One Charge Storage, and Possible Implications in the Origin of Life. Advanced Functional Materials, 2022, 32, .	14.9	14
89	Vapor sensor realized in an ultracompact polarization interferometer built of a freestanding porous-silicon form birefringent film. IEEE Photonics Technology Letters, 2003, 15, 834-836.	2.5	13
90	Tunable Transformation Between SnS and SnO <sub>x</sub> Nanostructures via Facile Anodization and Their Photoelectrochemical and Photocatalytic Performance. Solar Rrl, 2018, 2, 1800161.	5.8	13

#	Article	IF	CITATIONS
91	Morphology and strain control of hierarchical cobalt oxide nanowire electrocatalysts via solvent effect. Nano Research, 2020, 13, 3130-3136.	10.4	13
92	Strong, Ductile, and Tough Nanocrystal-Assembled Freestanding Gold Nanosheets. Nano Letters, 2022, 22, 822-829.	9.1	13
93	A sustained intravitreal drug delivery system with remote real time monitoring capability. Acta Biomaterialia, 2015, 24, 309-321.	8.3	12
94	Bestow metal foams with nanostructured surfaces via a convenient electrochemical method for improved device performance. Nano Research, 2016, 9, 2364-2371.	10.4	12
95	Solution-Based Comproportionation Reaction for Facile Synthesis of Black TiO <sub>2</sub> Nanotubes and Nanoparticles. ACS Applied Energy Materials, 2020, 3, 6087-6092.	5.1	12
96	Self-templated formation of twin-like metal-organic framework nanobricks as pre-catalysts for efficient water oxidation. Nano Research, 2022, 15, 2887-2894.	10.4	12
97	Efficient Ternary CdSSe Quantumâ€Dotâ€Sensitized Solar Cells based on MgOâ€coated TiO <sub>2</sub> Nanoparticles. Energy Technology, 2014, 2, 526-530.	3.8	10
98	Electrochemical fabrication and optical properties of porous tin oxide films with structural colors. Journal of Applied Physics, 2014, 116, .	2.5	9
99	Electrochemical Fabrication of Coaxial Wavyâ€Channel Ni <sup>III</sup> O(OH)/Ni Nanocomposites for Highâ€Performance Supercapacitor Electrode Materials. Energy Technology, 2013, 1, 478-483.	3.8	8
100	Triple-layer Fabry–Perot/SPP aluminum absorber in the visible and near-infrared region. Optics Letters, 2015, 40, 934.	3.3	8
101	Supervariate ceramics: biomineralization mechanism. Materials Today Advances, 2021, 10, 100144.	5.2	8
102	Waterâ€assisted sintering of silica: Densification mechanisms and their possible implications in biomineralization. Journal of the American Ceramic Society, 2022, 105, 2945-2954.	3.8	8
103	Tunable ultrathin dual-phase P-doped Bi2MoO6 nanosheets for advanced lithium and sodium storage. Nano Research, 2022, 15, 6128-6137.	10.4	8
104	Novel Form Birefringence Modeling for an Ultracompact Sensor in Porous Silicon Films Using Polarization Interferometry. IEEE Photonics Technology Letters, 2004, 16, 1546-1548.	2.5	7
105	Gradient TiO <sub>2</sub> nanotube arrays. Physica Status Solidi C: Current Topics in Solid State Physics, 2011, 8, 1812-1814.	0.8	7
106	Gradient TiO <sub>2</sub> Nanotube Arrays via Asymmetric Anodization. ECS Journal of Solid State Science and Technology, 2012, 1, M6-M9.	1.8	7
107	Two-Dimensional Electron Gas at the Spinel/Perovskite Interface: Suppression of Polar Catastrophe by an Ultrathin Layer of Interfacial Defects. ACS Applied Materials & Interfaces, 2020, 12, 42982-42991.	8.0	7
108	Anodic self-assembly method for synthesizing hierarchical FeS/FeOx hollow nanospheres. Journal of Power Sources, 2021, 484, 229268.	7.8	7

#	Article	IF	CITATIONS
109	Supervariate Ceramics: Gelatinous and Monolithic Ceramics Fabricated under Ambient Conditions. Advanced Engineering Materials, 0, , 2100866.	3.5	7
110	Doubly Doped BaZnOS Microcrystals for Multicolor Luminescence Switching. Advanced Optical Materials, 2022, 10, 2102430.	7.3	7
111	Encapsulating atomic molybdenum into hierarchical nitrogen-doped carbon nanoboxes for efficient oxygen reduction. Journal of Colloid and Interface Science, 2022, 620, 67-76.	9.4	7
112	Photonic porous siliconâ€based hybrid particles by softâ€lithography. Physica Status Solidi C: Current Topics in Solid State Physics, 2011, 8, 1754-1758.	0.8	6
113	Metallic rugate structures for near-perfect absorbers in visible and near-infrared regions. Optics Letters, 2012, 37, 3495.	3.3	6
114	Porous metal-based multilayers for selective thermal emitters. Optics Letters, 2012, 37, 4883.	3.3	6
115	Wide angle and narrow-band asymmetric absorption in visible and near-infrared regime through lossy Bragg stacks. Scientific Reports, 2016, 6, 27061.	3.3	6
116	Electrochemically fabricated nanovolcano arrays for SERS applications. Journal of Raman Spectroscopy, 2013, 44, 29-34.	2.5	5
117	Facile Surfactantâ€, Reductantâ€, and Ag Saltâ€free Growth of Ag Nanoparticles with Controllable Size from 35 to 660 nm on Bulk Ag Materials. Chemistry - an Asian Journal, 2021, 16, 2249-2252.	3.3	5
118	In situ surface-enhanced Raman spectroscopy monitoring of molecular reorientation in plasmon-mediated chemical reactions. Journal of Catalysis, 2022, 413, 527-533.	6.2	5
119	Anodic TiO <sub>2</sub> â€based porous photonic films. Physica Status Solidi (A) Applications and Materials Science, 2011, 208, 1389-1393.	1.8	4
120	Electrochemically Synthesized Porous Ag Double Layers for Surface-Enhanced Raman Spectroscopy Applications. Langmuir, 2019, 35, 6340-6345.	3.5	4
121	Ultrafine Nanoporous Gold <i>via</i> Thiol Compound-Mediated Chemical Dealloying. Journal of Physical Chemistry C, 2020, 124, 10026-10031.	3.1	4
122	Thermal and Nonthermal Effects in Plasmonâ€Mediated Electrochemistry at Nanostructured Ag Electrodes. Angewandte Chemie, 2020, 132, 6856-6859.	2.0	4
123	Surface-Plasmon-Assisted Growth, Reshaping and Transformation of Nanomaterials. Nanomaterials, 2022, 12, 1329.	4.1	4
124	Transformation of Freestanding Carbon-Containing Gold Nanosheets into Au Nanoparticles Encapsulated within Amorphous Carbon: Implications for Surface Modification of Complex-Shaped Materials and Structures. ACS Applied Nano Materials, 2021, 4, 5098-5105.	5.0	3
125	Liquefaction-induced plasticity from entropy-boosted amorphous ceramics. Applied Materials Today, 2021, 23, 101011.	4.3	3
126	Amorphous Highâ€Entropy Hydroxides of Tunable Wide Solar Absorption for Solar Water Evaporation. Particle and Particle Systems Characterization, 2021, 38, 2100094.	2.3	3

#	Article	IF	CITATIONS
127	Elastoâ€Capillary Manipulation of Freestanding Inorganic Nanosheets: An Implication for Nanoâ€Manufacturing of Lowâ€Dimensional Structures. Advanced Materials Interfaces, 2022, 9, .	3.7	3
128	TiO2-Based Nano-Wells for Fabricating Nanocrystals. Journal of Nanoscience and Nanotechnology, 2011, 11, 11059-11063.	0.9	2
129	Metal-based rugate filters with strong visible and near-infrared reflectivity. Applied Physics B: Lasers and Optics, 2012, 107, 669-673.	2.2	2
130	TiO2Nanotubes: Selective Removal of the Outer Shells of Anodic TiO2Nanotubes (Small 1/2013). Small, 2013, 9, 36-36.	10.0	2
131	Structural evolution of a Ni/NiOx based supercapacitor in cyclic charging-discharging: A polarized neutron and X-ray reflectometry study. Electrochimica Acta, 2018, 290, 118-127.	5.2	2
132	Bipolar Conduction and Giant Positive Magnetoresistance in Doped Metallic Titanium Oxide Heterostructures. Advanced Materials Interfaces, 2021, 8, 2002147.	3.7	2
133	Supervariate Ceramics: Gelatinous and Monolithic Ceramics Fabricated under Ambient Conditions. Advanced Engineering Materials, 2021, 23, .	3.5	2
134	Large-Scale Epitaxial Growth of Ultralong Stripe BiFeO3 Films and Anisotropic Optical Properties. ACS Applied Materials & Interfaces, 2022, , .	8.0	1
135	SSL Stripping Technique (DHCP Snooping and ARP Spoofing Inspection). , 2022, , .		1
136	Porous silicon vapor sensor based on polarization interferometry. , 0, , .		0
137	Metal-based photonic coatings from electrochemical methods. , 2010, , .		0
138	Facile Fabrication of Porous Nickel Films with Tunable Colors. Journal of the Electrochemical Society, 2012, 159, H928-H931.	2.9	0
139	Black TiO <sub>2</sub> Nanomaterials Through Electrochemical and Mechanical Methods. , 2017, , 33-47.		0
140	Elasto apillary Manipulation of Freestanding Inorganic Nanosheets: An Implication for Nanoâ€Manufacturing of Lowâ€Dimensional Structures (Adv. Mater. Interfaces 20/2022). Advanced Materials Interfaces, 2022, 9, .	3.7	0